



HAL
open science

Structural Transformations on Vitrification in the Fragile Glass-Forming System CaAl_2O_4

James W E Drewitt, Louis Hennet, Anita Zeidler, Sandro Jahn, Philip
Salmon, Daniel Neuville, Henry Fischer

► **To cite this version:**

James W E Drewitt, Louis Hennet, Anita Zeidler, Sandro Jahn, Philip Salmon, et al.. Structural Transformations on Vitrification in the Fragile Glass-Forming System CaAl_2O_4 . Physical Review Letters, 2012, 109 (23), 10.1103/physrevlett.109.235501 . insu-01905955

HAL Id: insu-01905955

<https://insu.hal.science/insu-01905955>

Submitted on 26 Oct 2018

HAL is a multi-disciplinary open access archive for the deposit and dissemination of scientific research documents, whether they are published or not. The documents may come from teaching and research institutions in France or abroad, or from public or private research centers.

L'archive ouverte pluridisciplinaire **HAL**, est destinée au dépôt et à la diffusion de documents scientifiques de niveau recherche, publiés ou non, émanant des établissements d'enseignement et de recherche français ou étrangers, des laboratoires publics ou privés.

Structural Transformations on Vitrification in the Fragile Glass-Forming System CaAl_2O_4

James W. E. Drewitt,^{1,2,*} Louis Hennet,² Anita Zeidler,³ Sandro Jahn,⁴ Philip S. Salmon,³
Daniel R. Neuville,⁵ and Henry E. Fischer⁶

¹Centre for Science at Extreme Conditions, School of Physics and Astronomy, University of Edinburgh,
Edinburgh EH9 3JZ, United Kingdom

²Conditions Extrêmes et Matériaux: Haute Température et Irradiation, CEMHTI-CNRS, Université d'Orléans,
1d avenue de la Recherche Scientifique, 45071 Orléans cedex 2, France

³Department of Physics, University of Bath, Bath BA2 7AY, United Kingdom

⁴GFZ German Research Centre for Geosciences, Telegrafenberg, 14473 Potsdam, Germany

⁵CNRS-IPGP, Géochimie et Cosmochimie, Sorbonne Paris Cité, 1 rue Jussieu, 75005 Paris, France

⁶Institut Laue Langevin, 6 rue Jules Horowitz, BP 156, 38042 Grenoble, France

(Received 3 September 2012; published 5 December 2012)

The structure of the fragile glass-forming material CaAl_2O_4 was measured by applying the method of neutron diffraction with Ca isotope substitution to the laser-heated aerodynamically levitated liquid at 1973(30) K and to the glass at 300(1) K. The results, interpreted with the aid of molecular dynamics simulations, reveal key structural modifications on multiple length scales. Specifically, there is a reorganization on quenching that leads to an almost complete breakdown of the AlO_5 polyhedra and threefold coordinated oxygen atoms present in the liquid, and to their replacement by a predominantly corner-sharing network of AlO_4 tetrahedra in the glass. This process is accompanied by the formation of branched chains of edge and face-sharing Ca-centered polyhedra that give cationic ordering on an intermediate length scale, where the measured coordination number for O around Ca is 6.0(2) for the liquid and 6.4(2) for the glass.

DOI: [10.1103/PhysRevLett.109.235501](https://doi.org/10.1103/PhysRevLett.109.235501)

PACS numbers: 61.05.fm, 61.20.-p, 61.43.Fs

Calcium aluminates $(\text{CaO})_x(\text{Al}_2\text{O}_3)_{1-x}$ ($0 \leq x \leq 1$) have been extensively studied on account of their geological, technological, and scientific importance [1–20]. For example, they are a significant component of the Earth's mantle so that the liquid structure is of interest for understanding magma-related processes [21], they are an integral component of aluminous cement [22], the glasses have a favorable infrared transmission window that extends up to a wavelength $\sim 6 \mu\text{m}$ [23] giving them optical applications [24,25], and the rare-earth-metal-doped materials exhibit persistent luminescence [26]. From a glass physics perspective, calcium aluminates are very *fragile* glass formers [1,4] and, in contrast to strong network glass formers such as SiO_2 , large structural alterations should accompany the rapid change in viscosity and other dynamical properties as the glass transition temperature T_g is approached [27]. Experimental information on the extent of structural transformation is therefore essential to understanding the processes occurring around T_g and the material properties to which they are linked. An experimental exploration of liquid aluminates is, however, challenging because of the high temperatures involved.

The containerless method of aerodynamic levitation offers a way forward, and by minimizing heterogeneous nucleation, it extends the narrow glass-forming region centered at $x = 0.65$ in the calcium aluminate system to include the equimolar composition CaAl_2O_4 [16] which has a fragility index of $m = 116$ [1,28]. At this composition, the O:Al ratio is 2:1 such that it is just feasible to form

an ideal network of fully connected corner-sharing AlO_4 tetrahedra where the oxygen atoms are twofold coordinated, as in the crystalline phase which has a tridymite-like structure where the tetrahedra form a fully polymerized network of six-membered rings [29]. This has motivated a range of experimental and computer simulation studies on the liquid and glass structure [2–20]. It has, however, proved difficult to measure unambiguously the Al and Ca coordination environments. For example, in the liquid state ^{27}Al nuclear magnetic resonance (NMR) experiments observe the fast exchange limit such that individual Al coordination environments cannot be identified [2–5], and in diffraction experiments, the nearest-neighbor Ca-O and other pair correlations are strongly overlapped [16–19]. The powerful method of neutron diffraction with isotope substitution has been used to probe directly the coordination environment of Ca in $(\text{CaO})_{48}(\text{SiO}_2)_{49}(\text{Al}_2\text{O}_3)_3$ glass [30,31], but the method is usually limited to large samples [32]. In this Letter we show, however, that the neutron diffraction with isotope substitution method can be used to measure the detailed atomic structure of a single aerodynamically levitated laser-heated drop of liquid CaAl_2O_4 at 1973(30) K. The structure of the glass at 300(1) K is also investigated. The results, interpreted with the aid of molecular dynamics (MD) simulations, characterize the nature of the structural transformations that occur on vitrification on *both* the local and intermediate atomic length scales.

The total structure factor measured by neutron diffraction is given by $F(Q) = \sum_{\alpha} \sum_{\beta} c_{\alpha} c_{\beta} b_{\alpha} b_{\beta} [S_{\alpha\beta}(Q) - 1]$,

where $S_{\alpha\beta}(Q)$ is a partial structure factor for chemical species α and β , Q is the magnitude of the scattering vector, while c_α and b_α are the atomic fraction and coherent neutron scattering length of chemical species α , respectively [32]. If three structurally identical samples of CaAl_2O_4 are prepared containing $^{\text{nat}}\text{Ca}$ [$b_{\text{nat}} = 4.70(2)$ fm [33]], predominantly ^{44}Ca [$b_{44} = 1.45(6)$ fm] or a 50:50 mixture of the two $^{\text{mix}}\text{Ca}$ [$b_{\text{mix}} = 3.08(3)$ fm], then the Ca correlations will receive different weighting factors and give rise to observably different $F(Q)$ functions. The $S_{\alpha\beta}(Q)$ with $\{\alpha, \beta\} \neq \text{Ca}$ will, however, receive identical weighting factors and can therefore be eliminated by taking a difference function such as

$$\begin{aligned}\Delta^{\text{Ca}}(Q) &\equiv {}^{\text{nat}}F(Q) - {}^{44}F(Q) \\ &= c_{\text{Ca}}^2(b_{\text{nat}}^2 - b_{44}^2)[S_{\text{CaCa}}(Q) - 1] \\ &\quad + 2c_{\text{Ca}}(b_{\text{nat}} - b_{44})\delta^{\text{Ca}}(Q),\end{aligned}\quad (1)$$

where $\delta^{\text{Ca}}(Q)$ involves only those $S_{\text{Ca}\beta}(Q)$ with $\beta \neq \text{Ca}$:

$$\delta^{\text{Ca}}(Q) = c_{\text{Al}}b_{\text{Al}}[S_{\text{CaAl}}(Q) - 1] + c_{\text{O}}b_{\text{O}}[S_{\text{CaO}}(Q) - 1],\quad (2)$$

$b_{\text{Al}} = 3.449(5)$ and $b_{\text{O}} = 5.803(4)$ fm [33]. Alternatively, the $S_{\text{Ca}\beta}(Q)$ with $\beta \neq \text{Ca}$ can be eliminated by taking a weighted difference function such as

$$\begin{aligned}\Delta^x(Q) &\equiv [b_{\text{nat}}{}^{44}F(Q) - b_{44}{}^{\text{nat}}F(Q)]/(b_{\text{nat}} - b_{44}) \\ &= \delta^x(Q) - c_{\text{Ca}}^2b_{\text{nat}}b_{44}[S_{\text{CaCa}}(Q) - 1],\end{aligned}\quad (3)$$

where $\delta^x(Q)$ involves only correlations with $\{\alpha, \beta\} \neq \text{Ca}$:

$$\begin{aligned}\delta^x(Q) &= c_{\text{Al}}^2b_{\text{Al}}^2[S_{\text{AlAl}}(Q) - 1] + c_{\text{O}}^2b_{\text{O}}^2[S_{\text{OO}}(Q) - 1] \\ &\quad + 2c_{\text{Al}}c_{\text{O}}b_{\text{Al}}b_{\text{O}}[S_{\text{AlO}}(Q) - 1].\end{aligned}\quad (4)$$

Moreover, $\delta^x(Q)$, $\delta^{\text{Ca}}(Q)$ and $S_{\text{CaCa}}(Q)$ can be extracted individually by solving the matrix equation

$$\begin{bmatrix} {}^{\text{nat}}F(Q) \\ {}^{\text{mix}}F(Q) \\ {}^{44}F(Q) \end{bmatrix} = \begin{bmatrix} c_{\text{Ca}}^2b_{\text{nat}}^2 & 2c_{\text{Ca}}b_{\text{nat}} & 1 \\ c_{\text{Ca}}^2b_{\text{mix}}^2 & 2c_{\text{Ca}}b_{\text{mix}} & 1 \\ c_{\text{Ca}}^2b_{44}^2 & 2c_{\text{Ca}}b_{44} & 1 \end{bmatrix} \times \begin{bmatrix} S_{\text{CaCa}}(Q) - 1 \\ \delta^{\text{Ca}}(Q) \\ \delta^x(Q) \end{bmatrix}.\quad (5)$$

The real-space difference functions, denoted by $\Delta G^{\text{Ca}}(r)$, $\delta G^{\text{Ca}}(r)$, $\Delta G^x(r)$, and $\delta G^x(r)$, are obtained by replacing each $S_{\alpha\beta}(Q)$ by its corresponding partial pair-distribution function $g_{\alpha\beta}(r)$ in Eqs. (1)–(4), respectively.

The samples were synthesized by melting mixed powders of Al_2O_3 ($\geq 99.9\%$) and $^{\text{nat}}\text{CaCO}_3$ ($\geq 99\%$) or $^{44}\text{CaCO}_3$ (99.2% enrichment) in a platinum crucible using the method described in Ref. [12]. The resulting ceramics were levitated with arcal gas (96.5% Ar, 3.5% O_2), melted using a CO_2 laser, and rapidly cooled by cutting the laser power [quench rate of ~ 420 K s $^{-1}$ at the melting point $T_{\text{mp}} = 1878$ K [16]

slowing to ~ 300 K s $^{-1}$ at $1.25T_g$ where $T_g = 1180(4)$ K [5,16]] to form optically transparent and colorless spherical glass samples of diameter 2.54(1) or 3.18(1) mm for the liquid and glass diffraction experiments, respectively. The samples gave Raman spectra with bands at 558 and 785 cm $^{-1}$ that are characteristic of CaAl_2O_4 glass [7].

The neutron diffractometer D4c [34] was employed with an incident wavelength of 0.4978(1) Å to give a wide Q range extending to 23.45 Å $^{-1}$. The liquid experiments used the aerodynamic-levitation and laser-heating setup described in Ref. [35]. Diffraction patterns were measured for the samples at 1973(30) K levitated with arcal gas, the empty levitator with a flow of gas, and a solid vanadium sphere of 3 mm diameter for calibration purposes. The glass experiments were made under vacuum. Diffraction patterns were measured for the samples resting on top of the levitator nozzle, for the empty levitator, and for a solid vanadium sphere of 4 mm diameter. Counting times were ~ 24 h for each sample. The atomic number density ρ is 0.0734(5) Å $^{-3}$ for the liquid [36] and, as measured using Archimedes' method, 0.0773(3) Å $^{-3}$ for the glass. The data were corrected and checked for self-consistency according to the methods described in Ref. [32], with sample attenuation factors calculated for the correct geometry [37]. The results are discussed by comparison with MD simulations of the liquid at 2500 K, previously reported in Ref. [19], and with new MD simulations of the glass at 300 K as prepared from the liquid in the NPT ensemble by using a quench rate of 10^{12} K s $^{-1}$ to give a material with $\rho = 0.0760(3)$ Å $^{-3}$. The interaction potentials for both models take into account anion polarizability and shape-deformation effects as well as the polarizability of the calcium cations [19,38].

The measured reciprocal-space and real-space difference functions are shown in Figs. 1 and 2. The first and second peaks in $\Delta G^x(r)$ and $\delta G^x(r)$ arise from nearest-neighbor Al-O and O-O correlations, respectively. For the liquid, they give distances of $r_{\text{AlO}} = 1.77(1)$ and $r_{\text{OO}} = 2.89(2)$ Å such that the mean $\angle \text{O} - \text{Al} - \text{O}$ bond angle is 108.9(5) $^\circ$ as compared to 109.47 $^\circ$ for a regular tetrahedron. The Al-O distance is consistent with a structure made predominantly from AlO_4 and AlO_5 polyhedra [39] such that the measured coordination number for O around Al, $\bar{n}_{\text{Al}}^{\text{O}} = 4.20(4)$, points to 80(4)% AlO_4 and 20(4)% AlO_5 units. A small tail on the Al-O peak at ~ 2 Å may, however, indicate a small fraction of AlO_6 units. For the glass, $r_{\text{AlO}} = 1.75(1)$ and $r_{\text{OO}} = 2.88(1)$ Å, giving a mean $\angle \text{O} - \text{Al} - \text{O}$ bond angle of 110.7(5) $^\circ$, and the measured coordination number $\bar{n}_{\text{Al}}^{\text{O}} = 4.04(3)$ points to 96(3)% AlO_4 and 4(3)% AlO_5 units. This is consistent with ^{27}Al multiple quantum magic angle spinning NMR results, which show a glass structure built from 96.5% AlO_4 tetrahedra and 3.5% AlO_5 polyhedra [10]. X-ray absorption near-edge structure spectroscopy experiments suggest that most of these tetrahedra are fully corner sharing [8].

The difference functions from MD are in good overall agreement with the diffraction results (Figs. 1 and 2). For

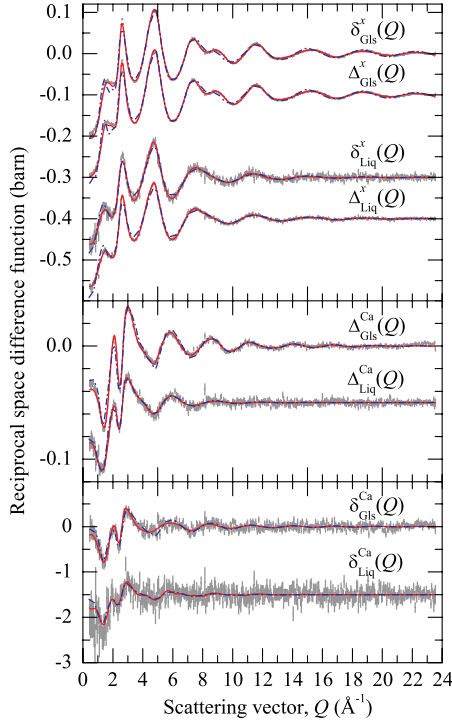


FIG. 1 (color online). The difference functions $\delta^x(Q)$, $\Delta^x(Q)$, $\Delta^{\text{Ca}}(Q)$, and $\delta^{\text{Ca}}(Q)$ for glassy (Gls) and liquid (Liq) CaAl_2O_4 . The vertical bars show the statistical errors on the measured data points, and the solid (red) curves show the back Fourier transforms of the corresponding real-space functions shown by the solid (black) curves in Fig. 2. The chained (blue) curves show the MD results. Several of the functions are displaced vertically for clarity of presentation.

the liquid, a largely tetrahedral structure is predicted with a significant fraction of AlO_5 units [14.7(5)%], many of which are edge sharing, and with small fractions of AlO_3 ($\leq 2\%$) and AlO_6 units ($\leq 0.4\%$). For the glass, a predominantly tetrahedral structure is predicted with a negligible fraction of AlO_3 units, 8.5(5)% AlO_5 units, and a few AlO_6 motifs ($\leq 0.4\%$). The concentration of AlO_5 units was found to be sensitive to the glass preparation method where a faster simulated quench rate of 10^{14} K s^{-1} gave a larger fraction of 14.0(5)%. The coordination number for Al around O is given by $\bar{n}_{\text{O}}^{\text{Al}} = (c_{\text{Al}}/c_{\text{O}})\bar{n}_{\text{Al}}^{\text{O}}$ [32]. For a system with the CaAl_2O_4 stoichiometry, the formation of units (e.g., AlO_4 and AlO_5) such that $\bar{n}_{\text{O}}^{\text{Al}} > 4$ will therefore lead to $\bar{n}_{\text{O}}^{\text{Al}} > 2$, i.e., a fraction of the oxygen atoms will take a coordination number in excess of two. If only twofold and threefold coordinated oxygen atoms can form, then the measured value $\bar{n}_{\text{O}}^{\text{Al}} = 2.10(2)$ for the liquid gives their fractions as 90(2)% and 10(2)%, respectively. In comparison, the MD simulations predict that 18(1)% of all O atoms exhibit a coordination number greater than two with 7(1)% forming oxygen triclusters, i.e., one oxygen atom shared by three AlO_4 tetrahedra [19,40]. Similarly, for the glass the measured value $\bar{n}_{\text{O}}^{\text{Al}} = 2.02(2)$ gives 98(2)% twofold and 2(2)% threefold coordinated oxygen atoms, while a study using ^{17}O – ^{27}Al heteronuclear

multiple quantum correlation NMR found that $\sim 5\%$ of the oxygen atoms form triclusters [9]. In comparison, the MD simulations find that 12(1)% of all O atoms exhibit a coordination number greater than two with 5(1)% forming oxygen triclusters. The latter play a more prominent role in the fragile glass former $\text{Ba}_2\text{Al}_6\text{O}_{11}$ where the O:Al ratio is less than two, such that there are insufficient oxygen atoms to form an ideal corner-sharing network of AlO_4 tetrahedra with twofold coordinated oxygen atoms. Instead, up to 21% of the oxygen atoms are involved in triclusters [41].

The first peak in $\Delta G^{\text{Ca}}(r)$ or $\delta G^{\text{Ca}}(r)$ is attributed to nearest-neighbor Ca-O correlations and, for the liquid, it gives a distance $r_{\text{CaO}} = 2.30(1) \text{ \AA}$ and coordination number $\bar{n}_{\text{Ca}}^{\text{O}} = 6.0(2)$ as found by using an integration cutoff of 3 \AA . For the glass, the corresponding values are $r_{\text{CaO}} = 2.35(1) \text{ \AA}$ and $\bar{n}_{\text{Ca}}^{\text{O}} = 6.4(2)$. These results are in good agreement with the MD simulations which find $r_{\text{CaO}} = 2.29(1) \text{ \AA}$ and $\bar{n}_{\text{Ca}}^{\text{O}} = 6.2(1)$ for the liquid [19] with $r_{\text{CaO}} = 2.34(1) \text{ \AA}$ and $\bar{n}_{\text{Ca}}^{\text{O}} = 6.4(1)$ for the glass. By comparison, the Ca atoms in crystalline CaAl_2O_4 stuff channels made from rings of corner-sharing AlO_4 tetrahedra to occupy two distorted octahedral sites and one ninefold-coordinated site such that

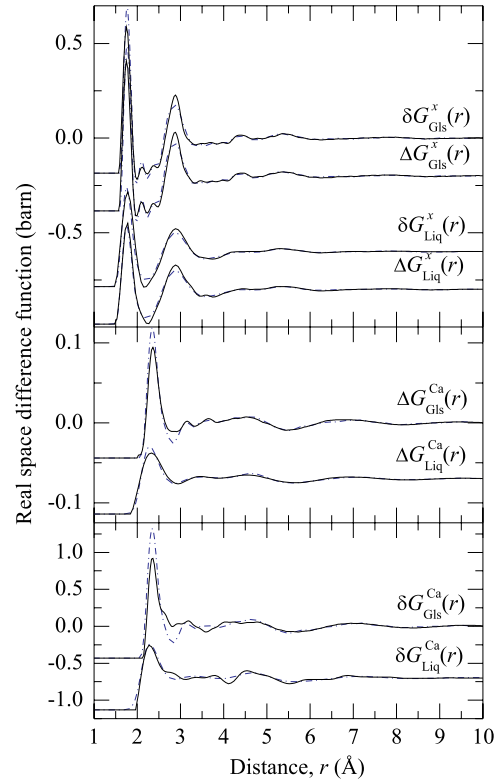


FIG. 2 (color online). The difference functions $\delta G^x(r)$, $\Delta G^x(r)$, $\Delta G^{\text{Ca}}(r)$, and $\delta G^{\text{Ca}}(r)$ for glassy (Gls) and liquid (Liq) CaAl_2O_4 as obtained by Fourier transforming the spline-fitted measured [solid (black) curves] or the simulated [chained (blue) curves] Q -space functions shown in Fig. 1. For clarity of presentation, the unphysical small- r oscillations below the distances of closest interatomic approach are omitted, and several of the functions are displaced vertically.

$\bar{n}_{\text{Ca}}^{\text{O}} = 7$ for $r \leq 3.18 \text{ \AA}$ [29]. In contrast, previous diffraction experiments on calcium aluminate liquids and glasses have consistently found much smaller $\bar{n}_{\text{Ca}}^{\text{O}}$ values, which have been explained by the obscuration of Ca-O correlations by other pair correlations at, e.g., large r in the glass [15–20,39,42]. Some success has been had in eliminating the O-O correlations by taking the difference between x-ray and neutron total structure factors, but coordination numbers of $\bar{n}_{\text{Ca}}^{\text{O}} = 3.8(3)$ [19] and $\bar{n}_{\text{Ca}}^{\text{O}} = 5.6(2)$ [15] are still obtained for liquid and glassy CaAl_2O_4 , respectively.

The measured $S_{\text{CaCa}}(Q)$ function for the glass is shown in Fig. 3 along with the partial pair-correlation function $d_{\text{CaCa}}(r) = 4\pi\rho r[g_{\text{CaCa}}(r) - 1]$. The latter exhibits two peaks at $r_{\text{CaCa}} = 3.59(2)$ and $4.41(5) \text{ \AA}$ and gives a coordination number $\bar{n}_{\text{Ca}}^{\text{Ca}} = 5.4(1)$ by integrating up to the minimum at 5.22 \AA . The simulated function has a single peak at $r_{\text{CaCa}} = 3.81(5) \text{ \AA}$ and yields a comparable coordination number of $\bar{n}_{\text{Ca}}^{\text{Ca}} = 4.9(1)$ by integrating up to the minimum at 5.09 \AA . The mean Ca-Ca distances for corner-, edge-, and face-sharing polyhedra are 4.40 , 3.74 , and 3.41 \AA , respectively. By comparison, crystalline CaAl_2O_4 has one Ca site with four Ca neighbors and two Ca sites with five Ca neighbors such that $\bar{n}_{\text{Ca}}^{\text{Ca}} = 4.7$ for distances in the range 3.55 – 4.99 \AA [29]. For the liquid, the smaller sample size precluded a reliable extraction of $S_{\text{CaCa}}(Q)$, but the MD results give $r_{\text{CaCa}} = 3.86(2) \text{ \AA}$ with $\bar{n}_{\text{Ca}}^{\text{Ca}} = 5.1(1)$ [19]. Overall, the MD simulations of the liquid and glass show that all Ca-centered polyhedra share at least one corner, but that there are larger numbers of edge-sharing and, to a lesser extent, face-sharing connections in the glass. This is

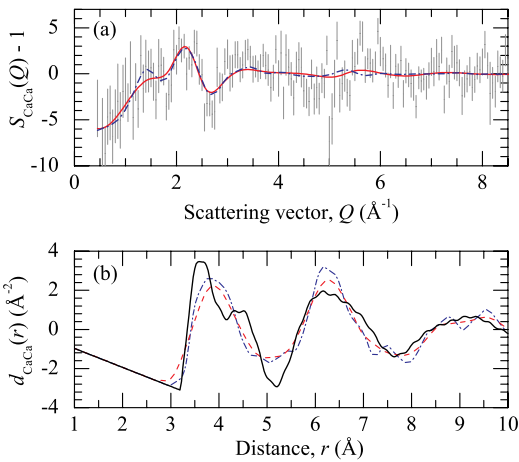


FIG. 3 (color online). (a) The measured (points with vertical error bars) and simulated [chained (blue) curve] partial structure factors $S_{\text{CaCa}}(Q)$ for CaAl_2O_4 glass. The solid (red) curve shows the back Fourier transform of $d_{\text{CaCa}}(r)$ given in (b) by the solid (black) curve. (b) The partial pair-correlation function $d_{\text{CaCa}}(r)$ as obtained by Fourier transformation of the spline-fitted measured [solid (black) curve] or the simulated [broken (red) curve] $S_{\text{CaCa}}(Q)$ function shown in (a) after applying a Lorch modification function with $Q_{\text{max}} = 8.5 \text{ \AA}^{-1}$. The chained (blue) curve shows the results obtained directly from the MD model.

illustrated in Fig. 4 for the case of edge-sharing polyhedra which form large branched chains in the glass as compared to the liquid. Indeed, on cooling the liquid the maximum cluster size increases significantly between 1500 and 1300 K ; in a regime where time-resolved studies indicate a change in the temperature dependence of the structure and thermal properties of liquid CaAl_2O_4 , perhaps marking a dynamical cross over at about $1.25T_g \approx 1475 \text{ K}$ [16].

We note that the Ca-Ca pair-correlation functions measured for CaAl_2O_4 glass (Fig. 3) are similar to those measured for $(\text{CaO})_{48}(\text{SiO}_2)_{49}(\text{Al}_2\text{O}_3)_3$ glass [31]. The latter were originally interpreted in terms of a structure comprising sheets of edge-sharing CaO_6 octahedra, a model that has subsequently been revised in favor of more chainlike linkages of Ca-centered polyhedra [43,44].

The following picture thus emerges for the significant structural changes that occur on both the local and intermediate length scales upon glass formation in the fragile CaAl_2O_4 system. On quenching, the AlO_5 polyhedra and threefold coordinated oxygen atoms found in the liquid reorganize to form a glass network made predominantly from corner-sharing AlO_4 tetrahedra. In this process there is a removal of Al-centered edge-sharing motifs, where the latter promote fragile behavior in glass forming systems [45]. The Ca-O coordination number shows a small increase from $6.0(2)$ to $6.4(2)$, and there is a large change in the connectivity of the Ca-centered polyhedra with the formation in the glass of branched chains involving edge- and face-sharing linkages.

Glasses can explore localities on an energy landscape that are inaccessible to the crystalline state and they are widely used as analogs for the liquid in materials of geophysical interest on account of the extreme conditions involved [21,46–50]. Although this is known to be an approximation [49,50], the nature of the problem makes it difficult to assess the extent of associated structural differences. The present work describes the reorganization on vitrification for a representative fragile glass former, a taxonomy that encompasses a range of magma-related liquids [51–53], and shows that significant changes occur not only in the character of the network-forming motifs but also in the nature of the intermediate ranged cationic ordering.

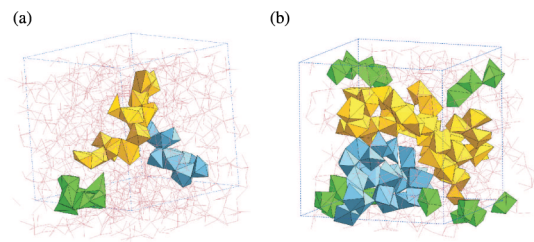


FIG. 4 (color online). Snapshots illustrating the largest clusters of edge-sharing Ca-centered polyhedra in the MD simulations of CaAl_2O_4 for (a) the liquid at 2500 K and (b) the glass at 350 K . The clusters are represented by the light (yellow), dark (blue), and medium (green) shaded units which involve 16 , 9 , and 8 Ca atoms in the liquid or 44 , 24 , and 19 Ca atoms in the glass, respectively.

We thank Gabriel Cuello and Alain Bertoni for help with the diffraction experiments. We also thank the French National Research Agency (ANR) (Grant No. NT09 432740), EPSRC (Grant No. EP/J009741/1), and DFG (Grant No. JA1469/4-1) for financial support, and acknowledge use of the EPSRC Chemical Database Service at Daresbury [54].

*james.drewitt@ed.ac.uk

- [1] G. Urbain, *Rev. Int. Hautes Tempér. Réfract. Fr.* **20**, 135 (1983).
- [2] B. Coté, D. Massiot, F. Taulelle, and J.-P. Coutures, *Chem. Geol.* **96**, 367 (1992).
- [3] B. T. Poe, P. F. McMillan, B. Coté, D. Massiot, and J.-P. Coutures, *Science* **259**, 786 (1993).
- [4] B. T. Poe, P. F. McMillan, B. Coté, D. Massiot, and J.-P. Coutures, *J. Am. Ceram. Soc.* **77**, 1832 (1994).
- [5] D. Massiot, D. Trumeau, B. Touzo, I. Farman, J.-C. Rifflet, A. Douy, and J.-P. Coutures, *J. Phys. Chem.* **99**, 16455 (1995).
- [6] P. F. McMillan, W. T. Petuskey, B. Coté, D. Massiot, C. Landron, and J.-P. Coutures, *J. Non-Cryst. Solids* **195**, 261 (1996).
- [7] I. Daniel, P. F. McMillan, P. Gillet, and B. T. Poe, *Chem. Geol.* **128**, 5 (1996).
- [8] D. R. Neuville, L. Cormier, A.-M. Flank, V. Briois, and D. Massiot, *Chem. Geol.* **123**, 153 (2004).
- [9] D. Iuga, C. Morais, Z. Gan, D. R. Neuville, L. Cormier, and D. Massiot, *J. Am. Chem. Soc.* **127**, 11540 (2005).
- [10] D. R. Neuville, L. Cormier, and D. Massiot, *Chem. Geol.* **229**, 173 (2006).
- [11] D. R. Neuville, L. Cormier, D. de Ligny, J. Roux, A.-M. Flank, and P. Lagarde, *Am. Mineral.* **93**, 228 (2008).
- [12] D. R. Neuville, G. S. Henderson, L. Cormier, and D. Massiot, *Am. Mineral.* **95**, 1580 (2010).
- [13] M. Licheron, V. Montouillout, F. Millot, and D. R. Neuville, *J. Non-Cryst. Solids* **357**, 2796 (2011).
- [14] S. A. Amin, K. Leinenweber, C. J. Benmore, R. Weber, and J. L. Yarger, *J. Phys. Chem. C* **116**, 2068 (2012).
- [15] C. J. Benmore, J. K. R. Weber, S. Sampath, J. Siewenie, J. Urquidi, and J. A. Tangeman, *J. Phys. Condens. Matter* **15**, S2413 (2003).
- [16] L. Hennes, I. Pozdnyakova, A. Bytchkov, D. L. Price, G. N. Greaves *et al.*, *J. Chem. Phys.* **126**, 074906 (2007).
- [17] L. Hennes, I. Pozdnyakova, V. Cristiglio, S. Krishnan, A. Bytchkov *et al.*, *J. Non-Cryst. Solids* **353**, 1705 (2007).
- [18] Q. Mei, C. J. Benmore, J. K. R. Weber, M. Wilding, J. Kim, and J. Rix, *J. Phys. Condens. Matter* **20**, 245107 (2008).
- [19] J. W. E. Drewitt, S. Jahn, V. Cristiglio, A. Bytchkov, M. Leydier, S. Brassamin, H. E. Fischer, and L. Hennes, *J. Phys. Condens. Matter* **23**, 155101 (2011); **24**, 099501 (2012).
- [20] Q. Mei, C. J. Benmore, J. Siewenie, J. K. R. Weber, and M. Wilding, *J. Phys. Condens. Matter* **20**, 245106 (2008).
- [21] S. Y. Park and S. K. Lee, *Geochim. Cosmochim. Acta* **80**, 125 (2012).
- [22] K. L. Scrivener and A. Capmas, *Lea's Chemistry of Cement and Concrete*, edited by P. C. Hewlett (Elsevier, Amsterdam, 1998), 4th ed., p. 713.
- [23] Y.-M. Sung and S.-J. Kwon, *J. Mater. Sci. Lett.* **18**, 1267 (1999).
- [24] M. E. Lines, J. B. MacChesney, K. B. Lyons, A. J. Bruce, A. E. Miller, and K. Nassau, *J. Non-Cryst. Solids* **107**, 251 (1989).
- [25] B. G. Aitken, M. J. Dejneka, and M. L. Powley, *J. Non-Cryst. Solids* **349**, 115 (2004).
- [26] T. Aitasalo, P. Dereń, J. Hölsä, H. Junger, J.-C. Krupa, M. Lastusaari, J. Legendziewicz, J. Niittykowsk, and W. Strek, *J. Solid State Chem.* **171**, 114 (2003).
- [27] C. A. Angell, *Science* **267**, 1924 (1995).
- [28] R. Böhmer, K. L. Ngai, C. A. Angell, and D. J. Plazek, *J. Chem. Phys.* **99**, 4201 (1993).
- [29] W. Hörkner and H. K. Müller-Buschbaum, *J. Inorg. Nucl. Chem.* **38**, 983 (1976).
- [30] M. C. Eckersley, P. H. Gaskell, A. C. Barnes, and P. Chieux, *Nature (London)* **335**, 525 (1988).
- [31] P. H. Gaskell, M. C. Eckersley, A. C. Barnes, and P. Chieux, *Nature (London)* **350**, 675 (1991).
- [32] H. E. Fischer, A. C. Barnes, and P. S. Salmon, *Rep. Prog. Phys.* **69**, 233 (2006).
- [33] V. F. Sears, *Neutron News* **3**, 26 (1992).
- [34] H. E. Fischer, G. J. Cuello, P. Palleau, D. Feltin, A. C. Barnes, Y. S. Badyal, and J. M. Simonson, *Appl. Phys. A* **74**, s160 (2002).
- [35] L. Hennes, I. Pozdnyakova, A. Bytchkov, V. Cristiglio, P. Palleau *et al.*, *Rev. Sci. Instrum.* **77**, 053903 (2006).
- [36] P. Courtial and D. B. Dingwell, *Geochim. Cosmochim. Acta* **59**, 3685 (1995).
- [37] A. Zeidler, *J. Appl. Crystallogr.* **45**, 122 (2012).
- [38] S. Jahn and P. A. Madden, *Phys. Earth Planet. Inter.* **162**, 129 (2007).
- [39] A. C. Hannon and J. M. Parker, *J. Non-Cryst. Solids* **274**, 102 (2000).
- [40] E. D. Lacy, *Phys. Chem. Glasses* **4**, 234 (1963).
- [41] L. B. Skinner, A. C. Barnes, P. S. Salmon, H. E. Fischer, J. W. E. Drewitt, and V. Honkimäki, *Phys. Rev. B* **85**, 064201 (2012).
- [42] E.-T. Kang, S.-J. Lee, and A. C. Hannon, *J. Non-Cryst. Solids* **352**, 725 (2006).
- [43] R. N. Mead and G. Mountjoy, *J. Phys. Chem. B* **110**, 14273 (2006).
- [44] C. J. Benmore, J. K. R. Weber, M. C. Wilding, J. Du, and J. B. Parise, *Phys. Rev. B* **82**, 224202 (2010).
- [45] M. Wilson and P. S. Salmon, *Phys. Rev. Lett.* **103**, 157801 (2009).
- [46] J. F. Stebbins and D. Sykes, *Am. Mineral.* **75**, 943 (1990).
- [47] G. S. Henderson, *Can. Mineral.* **43**, 1921 (2005).
- [48] W. E. Jackson, F. Farges, M. Yeager, P. A. Mabrouk, S. Rossano, G. A. Waychunas, E. I. Solomon, and G. E. Brown Jr., *Geochim. Cosmochim. Acta* **69**, 4315 (2005).
- [49] G. S. Henderson, G. Calas, and J. F. Stebbins, *Elements* **2**, 269 (2006).
- [50] J. F. Stebbins, E. V. Dubinsky, K. Kaneshashi, and K. E. Kelsey, *Geochim. Cosmochim. Acta* **72**, 910 (2008).
- [51] D. Giordano and D. B. Dingwell, *J. Phys. Condens. Matter* **15**, S945 (2003).
- [52] D. Giordano and J. K. Russell, *J. Phys. Condens. Matter* **19**, 205148 (2007).
- [53] D. Giordano, J. K. Russell, and D. B. Dingwell, *Earth Planet. Sci. Lett.* **271**, 123 (2008).
- [54] D. A. Fletcher, R. F. McMeeking, and D. Parkin, *J. Chem. Inf. Comput. Sci.* **36**, 746 (1996).